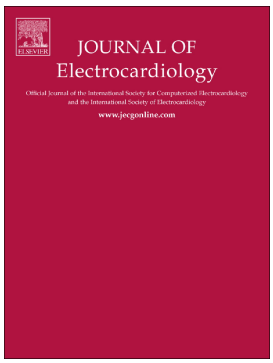

Electrocardiomatrix facilitates qualitative identification of diminished heart rate variability in critically ill patients shortly before cardiac arrest

Gang Xu, Sneha Dodaballapur, Temenuzhka Mihaylova, Jimo Borjigin

PII: S0022-0736(18)30348-0
DOI: doi:10.1016/j.jelectrocard.2018.08.006
Reference: YJELC 52690

To appear in: *Journal of Electrocardiology*

Please cite this article as: Gang Xu, Sneha Dodaballapur, Temenuzhka Mihaylova, Jimo Borjigin , Electrocardiomatrix facilitates qualitative identification of diminished heart rate variability in critically ill patients shortly before cardiac arrest. Yjelc (2018), doi:10.1016/j.jelectrocard.2018.08.006

Electrocardiomatrix facilitates qualitative identification of diminished heart rate variability in critically ill patients shortly before cardiac arrest

Short title: Electrocardiomatrix and heart rate variability

Author names and affiliations

Gang Xu[1], Sneha Dodaballapur[1], Temenuzhka Mihaylova[2], and Jimo Borjigin[1,2,3]

[1]Department of Molecular and Integrative Physiology, University of Michigan, Ann Arbor, MI, United States

[2]Department of Neurology, Michigan Medicine, Ann Arbor, MI, United States

[3]Michigan Center for Integrative Research in Critical Care, University of Michigan, Ann Arbor, MI, United States

Correspondence to:

Jimo Borjigin, PhD
Department of Molecular and Integrative Physiology
University of Michigan
7732C, Medical Science II
1137 E. Catherine St.
Ann Arbor, MI 48109-5622
borjigin@umich.edu

Acknowledgements

The authors would like to acknowledge Henry Lent and Fangyun Tian for their contributions to this work and the Department of Molecular and Integrative Physiology for support.

Competing Interests

The authors declare no competing interests.

Abstract

Background

Although heart rate variability (HRV) has diagnostic and prognostic value for the assessment of cardiac risk, HRV analysis is not routinely performed in a hospital setting. Current HRV analysis methods are primarily quantitative; such methods are sensitive to signal contamination and require extensive post hoc processing.

Methods and Results

Raw electrocardiogram (ECG) data from the Sleep Heart Health Study was transformed into electrocardiomatrix (ECM), in which sequential cardiac cycles are aligned, in parallel, along a shared axis. Such juxtaposition facilitates the visual evaluation of beat-to-beat changes in the R-R interval without sacrificing the morphology of the native ECG signal. Diminished HRV, verified by traditional methods, was readily identifiable. We also examined data from a cohort of hospitalized patients who suffered cardiac arrest within 24 hours of data acquisition, all of whom exhibited severely diminished HRV that were visually apparent on ECM display.

Conclusions

ECM streamlines the identification of depressed HRV, which may signal deteriorating patient condition.

Keywords

electrocardiomatrix, heart rate variability, cardiac arrest

Introduction

Heart rate variability (HRV) describes beat-to-beat changes in the length of the R-R interval (RRI) between normal sinus heartbeats. The precise mechanistic physiology behind HRV has yet to be fully elucidated. However, certain HRV functions are thought to reflect accelerated sympathetic nervous system activity, reduced parasympathetic activity, or both [1]. Specifically, accelerated sympathetic activity appears to drive a reduction in overall HRV. Reduced HRV is a known predictor of poor outcome in cases of ischemic stroke [2], sepsis [3], multiple organ dysfunction syndrome [4], myocardial infarction [5-8], and heart failure [9,10]. The manifestation of HRV abnormalities may also be a marker of clinical complications following acute stroke [11-13] and may signal the onset of dangerous ventricular dysrhythmias in cardiac patients [14,15]. Furthermore, studies using animal models of ischemic stroke [16] and sepsis [17] have suggested that measurable reductions in overall HRV appear to develop in advance of other abnormal clinical signs.

Despite its potential diagnostic and prognostic utility, HRV is not routinely analyzed in a healthcare setting. This sparse adoption may be attributed to a number of factors, many of which are associated with current methods of data processing and HRV measurement. First, inferences regarding autonomic activity can only be derived from HRV analysis if the measured RRIs fall between heartbeats originating from the sinoatrial node. Thus, in the context of HRV analysis, the presence of atrial and subatrial ectopy constitutes data contamination [18]. A number of algorithmic methods exist for the purpose of correcting electrocardiogram (ECG) data featuring signal artifact and/or ectopy. Although these methods may be used to prepare suboptimal data for HRV analysis, they generally rely on the deletion of aberrant electrical activity, either with or without subsequent interpolation. The extent to which these procedures compromise the ability of the data to represent the subject's true HRV depends on the severity of the contamination and the length of the recording [19]. In a subject with significant ectopic burden, the raw ECG recording may require substantial algorithmic alteration. What's more, the validity of any automated data correction must be manually verified by a trained technician. Manual review is not only time consuming; it prevents the implementation of HRV analysis as a tool for real time assessment of autonomic tone and clinical condition.

In addition to the complex problem of appropriate post hoc processing, the widespread use of HRV analysis as a clinical marker is hampered by strict data acquisition constraints. Although HRV

measurements may be derived from a typical ECG recording, subjects are usually placed in a supine position and instructed to remain still for the duration of the recording. In healthy subjects, data collected in this manner appears to provide valid, reproducible HRV measurements, especially when controlled breathing protocols are utilized [20]. However, such a protocol may be impractical for the measurement of HRV in critically ill or distressed patients, or patients who are otherwise unable to cooperative with the clinician. Moreover, HRV is best considered in a longitudinal manner [21] and may offer greater predictive power when measured over longer durations [22]. In order to effectively track patient progress, multiple, serial HRV measurements would need to be procured during the course of the patient's hospital stay. Given current data processing methods described above, widespread implementation of HRV analysis for real time patient monitoring in a hospital setting is not feasible. Given these short comings with the current HRV analytic approaches, a new method that allows one-glance estimation of patients' HRV status and permit real time monitoring of their HRV trend is expected to facility the use of HRV in clinical practice.

Here, we describe a method for qualitative, visual assessment of overall HRV in real time without the need for artifact correction, post hoc processing, or the imposition of strictly controlled conditions. Electrocardiomatrix (ECM) is a new technique for the efficient assessment of lengthy sections of ECG data without compromising signal morphology or resolution. ECM facilitates the single-glance identification of decreased HRV even in the presence of ectopic contamination, signal noise, or incorrectly annotated R peaks.

Methods

ECM construction

ECM has been previously described and validated for the evaluation of cardiac dysrhythmias [23]. ECM is a representation of electrophysiological signals constructed in an automated fashion from standard ECG data. R peaks are detected via a modified variable threshold algorithm and peak selection is subsequently interpreted via a graphical user interface.

The construction of the ECM heat map from a short section of representative ECG is illustrated in Figure 1. First, the ECG recording (panel A) is divided into short segments, each containing at least two adjacent heartbeats (panel B). The duration of the constituent segments may be adjusted to ensure two

consecutive heartbeats remain in frame regardless of heartrate. The first R peak is situated at time 0, such that the corresponding P wave remains visible in frame. The second R peak in the first time segment assumes the time 0 position in the second segment. Subsequent time segments are aligned along the first of their two R peaks. The entire series of ECG segments is transformed into a colorimetric heat map, such that positive voltage deflections are represented by warmer colors (red) and negative deflections are represented by cooler colors (blue). The resulting ECM consists of consecutive R-R intervals aligned in parallel along a shared axis (panel C). The juxtaposition of sequential time segments with partial overlap exposes very subtle beat-to-beat changes in RRI and other important ECG intervals (PR, QT, and ST) (panel D) that may be difficult to discern from a traditional ECG tracing (panel A).

ECM-based visual estimation of HRV

In a completed ECM panel, at least two rows of heartbeats should be visible: the R^n row, invariably positioned at time 0, and the R^{n+1} row (panel E). The R^n row should always be a straight line, as determined by the ECM algorithm, whereas the appearance of the R^{n+1} row varies, depending on the extent of HRV. If HRV is extremely low or absent, these two rows will appear completely parallel. In the subject shown in Figure 1, HRV is readily visible. Thus, ECM allows users to rapidly formulate an overall impression of HRV as soon as the matrix is formed, even when artifacts or noise are present in patients' ECG data (see Figure 4 below).

Data sourcing

We examined data from the Sleep Heart Health Study (SHHS) [24], a prospective cohort study principally designed to examine the relationship between sleep disordered breathing and cardiovascular disease. In total, the study includes 6441 participants, all aged 40 years and older. Participants underwent in-home polysomnography (PSG) including continuous three-lead ECG and chin electromyogram (EMG) [25,26]. ECG data were recorded in modified Einthoven lead II (MLII) at a sample frequency of 250 Hertz. The SHHS attempted to collect a full night of ECG data from each subject. The length of the recordings ranges from approximately 6-13 hours, depending on the success of signal acquisition and the time each subject spent in bed. For our study, a total of four hours of data were considered from each subject, beginning at the moment of sleep onset. Onset time varies widely among subjects, and HRV values collected during subsequent periods of nighttime wakefulness were not excluded.

Additional ECG recordings were obtained from critically ill, adult patients admitted to the Neurological Intensive Care Unit (NICU) at the University of Michigan (UM), five of whom showed high-quality data suitable for quantitative data analysis. NICU patient ECG data was recorded at a sample frequency of 512 Hertz in MLII.

HRV analysis

The SHHS selected 495 overnight ECGs for HRV analysis. The complete ECG recordings were divided into five-minute segments for HRV analysis. The SHHS performed quantitative HRV analysis on each 5-minute segment beginning at the time of sleep onset and continuing until termination of signal [25]. From this cohort, we identified 493 participants suitable for comparison with critically ill NICU patients. Two participants were excluded for having fewer than four hours of sleep time, rendering them unsuitable for comparison to the four-hour recordings collected from the NICU patients. Our study is principally concerned with the standard deviation of all normal-to-normal intervals (SDNN).

We processed four hours of ECG data preceding cardiac arrest in hospitalized patients from the UM-NICU. NICU patients' ECG data was divided into consecutive 30-minute epochs, terminating at the loss of signal. From each of eight 30-minute epochs, a 5-minute section with minimal artifact and ectopic contamination was selected for quantitative HRV analysis. Effort was taken to identify suitable 5-minute segments from the beginning of each epoch, in order to confer the greatest degree of sampling regularity. This screening process was performed with the aid of ECM. Signal artifact and ectopic beats, where present, were addressed through simple deletion of the affected RRIs using methods described by Kaufmann et al. [27]. Quantitative analysis was performed for 5-minute segments within each 30-minute epoch until loss of signal or the onset of ventricular tachycardia, ventricular fibrillation, profound bradycardia (less than 40 beats per minute), or $2^{nd}/3^{rd}$-degree atrioventricular block. Each of the five patients suffered cardiac arrest within 24 hours following the end of their recording.

Statistical analysis

SDNN values from NICU patients and SHHS patients were compared using a two-sample Student's t-test assuming unequal variances.

Results

SHHS participants were sorted according to SDNN. This study was primarily concerned with the translation of traditional quantitative HRV measurements to observable morphological features within the corresponding ECM heat map. Accordingly, eight 5-minute sections of ECG data from participants with known SDNN were transformed into ECM. No single participant provided more than one 5-minute section for analysis. We selected four participants known to have very low SDNN and four participants known to have mean SDNN values. SDNN values for these subjects are shown in Table 1, including those reported by SHHS and those produced by our own independent analysis. Our measured SDNN values and those reported by SHHS differ only slightly. We attribute these differences to slight variations in R peak labeling between our detection algorithm [23] and that used by SHHS.

By design, the ECM is constructed such that the R^n peaks of each time segment are uniformly aligned at time 0 seconds. Consequently, the bottom R^n row of R peaks forms a uniform, straight line of high colorimetric intensity (red/yellow). In subjects with normal HRV, no such alignment is present in the upper row of R-peaks (R^{n+1}) (Figure 1E). In fact, participants (#1-4) with moderate to high SDNN values show consistent variations in RRI that are visible upon inspection of the ECM (Figure 2A). Low-SDNN participants (#5-8), however, produce ECM images exhibiting strikingly uniform alignment of the R^{n+1}-peaks. In subjects with extremely diminished HRV, the upper row of R^{n+1}-peaks adopts such severe uniformity that it begins to appear parallel with the bottom row of R^n-peaks (Figure 2B). This feature is common to all of the low-SDNN participants and is a direct reflection of the extreme RRI consistency quantified by the corresponding SDNN value. Note that values reported in Table 1 are measurements taken from 5-minute segments of data, but the corresponding ECM images in Figure 2 display only two minutes of each 5-minute segment. ECM images were shortened for efficient presentation and side-by-side comparison.

In order to validate the utility of ECM for the assessment of HRV in hospitalized patients, we examined pre-arrest ECG data from a small cohort of NICU patients. SDNN values measured are significantly and persistently depressed in critical patients compared to outpatient SHHS participants (Figure 3A). Average 5-minute HRV values, sampled from every 30-minute epoch for the duration of the four-hour recording, were calculated (Table 2). We also collected longitudinal, 5-minute ECM images from ICU patients in order to determine if measurable changes in HRV could be perceptible using ECM, alone. Representative images from Patient D, collected during the hours prior to cardiac arrest, appear to display a gradual

decline in HRV towards the end of the recording (Figure 3B). The patient's time of death was marked in the electronic medical record at 3:28 PM.

Erroneous algorithmic peak annotation, difficult to detect in traditional HRV analysis based solely on ECG raw data, can be a source of artefact that would affect HRV analysis. In contrast, misidentified R peaks are readily and clearly visible upon viewing ECM, since they precipitate an obvious irregularity in the Rn line of peaks (Figure 4A). Normally, Rn peaks are aligned with perfect uniformity. Regardless of the detection algorithm used, undetected peaks present as gaps in the Rn row. Incorrect R peak detection will also disrupt the uniformity of the Rn alignment and draw the attention of the viewer. In this figure (upper panel), black arrows correspond to the detected peaks. In this particular case, three T waves have labeled as R peaks. This error creates a striking abnormality in the Rn row, which can then be corrected, if desired (Figure 4A). In this particular example, we had R-peaks purposefully labelled on the T-waves to show how misidentified R peaks appear on ECM. In reality, misidentification of R peaks occurs more commonly when the T-waves are tall and peaked.

The presence of arrhythmic beats in ECG signal, which must be removed manually in traditional methods of HRV analysis, can also constitute the source for artefact that affect HRV analysis. To demonstrate how heart period fluctuation appears on ECM for signals with arrhythmic beats, we selected a 5-minute segment of NICU ECG data with multiple premature atrial contractions (PACs; Figure 4B). For this particular segment, the uncorrected SDNN was found to be 35.92 ms. When corrected by simple deletion of the affected RRIs, the true SDNN was found to be 2.31 ms. This example shows just how wildly the presence of arrhythmias can change the values of HRV, if left uncorrected. In contrast, the marked parallel alignment of the R^n and R^{n+1} peaks, a qualitative marker of reduced HRV on ECM, is not disrupted, and the low HRV remains visually apparent on the ECM display (lower panel). This data shows that ECM-based visual HRV estimation is less influenced by the presence of arrhythmia.

Discussion

ECM enables single-glance inspection of large amounts of electrophysiological data. While such functionality has applications in dysrhythmia identification, this paper focuses on the use of ECM to assess and monitor HRV without relying on traditional methods of quantitative analysis. Previous methods of HRV analysis have not seen widespread clinical use, possibly due to lengthy data processing

times and the lack of robust methods for artifact correction [18]. In many cases, ECM-mediated analysis effectively bypasses the need for HRV quantification, while still providing a faithful representation of the subject's overall HRV. Furthermore, continuous ECM streaming, which can be easily added to any ECG monitoring device, allows real time evaluation of cardiac signals in a manner akin to the ubiquitous ECG, and permit visual identification of transient cardiac events such as minibursts in heart period fluctuations that link heartbeats to other physiological events [28].

Generally, ECG data that is heavily contaminated with ectopy or musculoskeletal noise is not suitable for HRV analysis without manual correction [18]. These constraints are likely to be particularly relevant in seriously ill patients in a hectic ICU setting, where baseline tremors, abnormal respirations, and altered mental status may hinder the acquisition of ideal data. However, since ECM-mediated HRV analysis is qualitative and does not rely on sensitive algorithmic processing, we are able to demonstrate its utility for the inference of overall HRV in unedited ECG recordings with various ectopic beats and signal artifact. The presence of premature ventricular contractions (PVCs) or PACs does not significantly disrupt the underlying ECM morphology. Upon inspection of the ECM, even a heavy ectopic burden does not obfuscate the variability of the underlying sinus rhythm. Similarly, signal noise attributable to musculoskeletal activity causes a local disruption in the quality of the cardiac signal but does not compromise the ability of a discerning analyst to develop an impression of the subject's HRV on ECM. Notably, if quantitative analysis is desired, manual correction is still required. However, ECM expedites the process by allowing the compact evaluation of long ECG recordings and enhancing the appearance of algorithmic errors. Thus, while quantitative HRV reporting is likely indispensable, ECM-mediated HRV analysis may be a viable and useful addition to the existing repertoire of methods for monitoring patient progress and directing the clinical treatment plan. It must be noted, however, ECM-based HRV survey requires human eye interpretation, and automatic interpretation remains challenging at this point.

As a reflection of sympathetic tone, HRV may signal impending cardiovascular events in hospitalized patients. We obtained ECG data from a small cohort of hospitalized, critically ill patients who subsequently suffered in-hospital cardiac arrest. All of these patients exhibited persistent reduction in SDNN during the hours immediately preceding cardiac arrest. Although these findings are only preliminary and the etiology of such HRV changes is largely unknown, sympathetic overdrive has been implicated in the pathophysiology of heart failure and is, itself, associated with poor outcome in heart failure patients [29]. Importantly, our initial evaluation in prearrest patients reveals reduced HRV that

appears to manifest independent of tachycardia, an accepted metric for gauging the severity of heart failure-associated sympathetic dysfunction [30,31]. Thus, the progress of HRV changes may offer an additional indicator of cardiac function and treatment efficacy.

It must be noted that our analysis only considered NICU patients who ultimately suffered in-hospital cardiac arrest. We were unable to source data from an analogous cohort of critically ill patients with favorable outcomes. Thus, based on the results of this study, alone, we are not able to establish a strong correlation between diminished HRV and poor outcome. In addition, we were not able to obtain clinical event data for the recording period. It is, therefore, impossible to isolate the effects of treatment interventions on cardiac electrophysiology. Furthermore, the onset of an arrest rhythm is only captured in one of our five NICU recordings. All other patients were removed from monitoring for a number of hours prior to the time of death. Thus, we do not capture sufficient data to draw conclusions about HRV during the period immediately preceding cardiac arrest. Future studies ought to collect longer recordings and aim to capture the moment of cardiac arrest. The longitudinal ECM images shown for Patient D in Figure 3B do appear to capture a declining trend in overall HRV. However, such a trend was not visually apparent upon examination of the ECM images from the other four NICU patients, which appeared only to display persistently low HRV. We are, therefore, unable to conclude that declining HRV is a development signaling imminent cardiac arrest.

Nevertheless, our results do suggest diminished HRV is associated with life-threatening illness, with near-death patients consistently exhibiting SDNN values well below those of outpatients. It is also worth noting that, although none were sufficiently ill at the time of PSG to merit hospitalization, many participants in the SHHS cohort do have significant medical history. Thus, HRV measurements taken from a completely healthy population would, potentially, contrast even more starkly with HRV observed in ICU patients.

In conclusion, our data suggest that ECM can promote qualitative and visual assessment of overall HRV and facilitates the single-glance identification of decreased HRV even in the presence of ectopic contamination or signal noise. These features may support the use of the HRV in clinical practice.

References

1. Cygankiewicz I, Zareba W. Heart rate variability. Handbook of Clinical Neurology 117:379, 2013
2. Tang S-C, Jen H-I, Lin Y-H et al. Complexity of heart rate variability predicts outcome in intensive care unit admitted patients with acute stroke. Journal of Neurology, Neurosurgery, and Psychiatry 86:95, 2015
3. de Castilho FM, Ribeiro ALP, da Silva JLP et al. Heart rate variability as predictor of mortality in sepsis: A prospective cohort study. PloS One 12:e0180060, 2017
4. Schmidt H, Müller-Werdan U, Hoffmann T et al. Autonomic dysfunction predicts mortality in patients with multiple organ dysfunction syndrome of different age groups. Critical Care Medicine 33:1994, 2005
5. Kleiger RE, Miller JP, Bigger JT et al. Decreased heart rate variability and its association with increased mortality after acute myocardial infarction. The American Journal of Cardiology 59:256, 1987
6. Bigger JT, Kleiger RE, Fleiss JL et al. Components of heart rate variability measured during healing of acute myocardial infarction. The American Journal of Cardiology 61:208, 1988
7. Stein PK, Domitrovich PP, Huikuri HV et al. Traditional and nonlinear heart rate variability are each independently associated with mortality after myocardial infarction. Journal of Cardiovascular Electrophysiology 16:13, 2005
8. Song T, Qu XF, Zhang YT et al. Usefulness of the heart-rate variability complex for predicting cardiac mortality after acute myocardial infarction. BMC cardiovascular disorders 14:59, 2014
9. Bilchick KC, Fetics B, Djoukeng R et al. Prognostic value of heart rate variability in chronic congestive heart failure (Veterans Affairs' Survival Trial of Antiarrhythmic Therapy in Congestive Heart Failure). The American Journal of Cardiology 90:24, 2002
10. Hadase M, Azuma A, Zen K et al. Very low frequency power of heart rate variability is a powerful predictor of clinical prognosis in patients with congestive heart failure. Circulation Journal: Official Journal of the Japanese Circulation Society 68:343, 2004
11. Chen W-L, Kuo C-D. Characteristics of heart rate variability can predict impending septic shock in emergency department patients with sepsis. Academic Emergency Medicine: Official Journal of the Society for Academic Emergency Medicine 14:392, 2007
12. Günther A, Salzmann I, Nowack S et al. Heart rate variability - a potential early marker of sub-acute post-stroke infections. Acta Neurologica Scandinavica 126:189, 2012
13. Chen C-H, Huang P-W, Tang S-C et al. Complexity of Heart Rate Variability Can Predict Stroke-In-Evolution in Acute Ischemic Stroke Patients. Scientific Reports 5:17552, 2015
14. Huikuri HV, Koistinen MJ, Yli-Mäyry S et al. Impaired low-frequency oscillations of heart rate in patients with prior acute myocardial infarction and life-threatening arrhythmias. The American Journal of Cardiology 76:56, 1995
15. Lombardi F. Altered heart rate variability patterns preceding ventricular tachycardia. Cardiology Review 18:35, 2001
16. Kodata T, Kamata K, Fujiwara K et al. A new infarction detection method based on heart rate variability in rat middle cerebral artery occlusion model. Conference proceedings: Annual International Conference of the IEEE Engineering in Medicine and Biology Society IEEE Engineering in Medicine and Biology Society Annual Conference 2017:3061, 2017
17. Jarkovska D, Valesova L, Chvojka J et al. Heart-rate variability depression in porcine peritonitis-induced sepsis without organ failure. Experimental Biology and Medicine (Maywood, NJ) 242:1005, 2017
18. Peltola MA. Role of editing of R-R intervals in the analysis of heart rate variability. Frontiers in Physiology 3:148, 2012

19. Rincon Soler AI, Silva LEV, Fazan R et al. The impact of artifact correction methods of RR series on heart rate variability parameters. Journal of Applied Physiology (Bethesda, Md: 1985)jap.00927.2016, 2017
20. Pinna GD, Maestri R, Torunski A et al. Heart rate variability measures: a fresh look at reliability. Clinical Science (London, England: 1979) 113:131, 2007
21. Malik M, Bigger JT, Camm AJ et al. Heart rate variabilityStandards of measurement, physiological interpretation, and clinical use. European Heart Journal 17:354, 1996
22. Shaffer F, McCraty R, Zerr CL. A healthy heart is not a metronome: an integrative review of the heart's anatomy and heart rate variability. Frontiers in Psychology 5:1040, 2014
23. Li D, Tian F, Rengifo S et al. Electrocardiomatrix: A new method for beat-by-beat visualization and inspection of cardiac signals. Journal of Integrative Cardiology 1, 2015
24. Dean DA, Goldberger AL, Mueller R et al. Scaling Up Scientific Discovery in Sleep Medicine: The National Sleep Research Resource. Sleep 39:1151, 2016
25. Quan SF, Howard BV, Iber C et al. The Sleep Heart Health Study: design, rationale, and methods. Sleep 20:1077, 1997
26. Redline S, Sanders MH, Lind BK et al. Methods for obtaining and analyzing unattended polysomnography data for a multicenter study. Sleep Heart Health Research Group. Sleep 21:759, 1998
27. Kaufmann T, Sütterlin S, Schulz SM et al. ARTiiFACT: a tool for heart rate artifact processing and heart rate variability analysis. Behavior Research Methods 43:1161, 2011
28. Roach D, Sheldon R. Origins of the power of the low frequency heart rate variability bandwidth. Journal of Electrocardiology 51:422, 2018
29. Devgun J, Jobanputra YB, Arustamyan M et al. Devices and interventions for the prevention of adverse outcomes of tachycardia on heart failure. Heart Failure Reviews, 2018
30. Böhm M, Swedberg K, Komajda M et al. Heart rate as a risk factor in chronic heart failure (SHIFT): the association between heart rate and outcomes in a randomised placebo-controlled trial. The Lancet 376:886, 2010
31. Swedberg K, Komajda M, Böhm M et al. Ivabradine and outcomes in chronic heart failure (SHIFT): a randomised placebo-controlled study. The Lancet 376:875, 2010

Table 1.

HRV was validated quantitatively for eight subjects from the Sleep Heart Health Study (SHHS). From the SHHS dataset of 495 subjects for which HRV measurements were obtained, four were selected with extremely low standard deviation of all normal-to-normal intervals (SDNN) values. An additional four subjects were selected for their proximity to the mean SDDN for the dataset. SDNN values were measured from a 5-minute section of ECG data. The absolute time marking the start of each section is reported in seconds. Measured values for each 5-minute segment are displayed alongside those reported by the SHHS in their publicly available dataset. All SDNN values were measured in milliseconds.

Subject	SHHS ID	Start time (s)	HRV Appearance	SDNN Measured (ms)	SDNN Reported (ms)[25]	Difference (ms)
1	203853	25320	Normal	52.22	52.24	0.01
2	205086	9480	Normal	52.18	52.24	0.06
3	200116	29820	Normal	52.28	52.23	0.05
4	205587	19500	Normal	55.13	52.24	2.90
5	200978	9060	Low	6.57	4.70	1.87
6	203424	7890	Low	2.86	2.91	0.06
7	204587	19860	Low	7.86	8.15	0.29
8	204865	10680	Low	6.45	6.31	0.13

Table 2.

Average HRV measurements were obtained for each NICU patient over a four-hour recording shortly before cardiac arrest. Each reported value represents the simple average of all 5-minute segments from a total of eight 30-minute epochs. We measured the mean R-R interval (mean RRI), SDNN, and root mean square of successive difference between R-R intervals (RMSSD). The mean instantaneous heart rate (mean IHR) was calculated from the mean RRI value.

Patient	Mean RRI (ms)	Mean IHR (beats/min)	SDNN (ms)	RMSSD (ms)
A	668.18	89.80	8.12	3.28
B	709.83	84.53	2.09	2.89
C	762.00	78.74	5.37	2.95
D	809.87	74.09	18.46	9.09
E	618.64	96.99	7.33	4.06

Figure Legends

Figure 1. ECM preserves ECG signal morphology while conveniently juxtaposing consecutive RR-intervals (RRI). A traditional ECG (panel **A**) displays beat-to-beat variations in the RRI, a normal phenomenon known as HRV. Although this RRI variation is difficult to meaningfully assess when viewing a traditional ECG strip, it becomes apparent when overlaying sequential interbeat intervals (panel **B**). Sequential RRIs, arranged in this way, are converted to a colorimetric heat map (panel **C**) to enable efficient evaluation of large sections of data containing many heartbeats. In panel **D**, the morphology of the ECG signal is completely preserved and beat-to-beat variations in RRI are perceptible. In this example, which contains six pairs of sequential cardiac cycles, the P wave and T wave are denoted by bands of light blue and light green colorimetric intensity, respectively. Thus, the ECM also allows at-a-glance evaluation of QT internal, PR interval, and ST segment dynamics. This very short section of ECM was extracted from a greater collection of cardiac signals (panel **E**), the examination of which reveals the highly dynamic nature of the RRI. Panels A-D are modified from Li et al. **[23].**

Figure 2. ECM facilitates visual interpretation of overall HRV. ECM images, each two-minutes in length, were constructed from Sleep Heart Health Study (SHHS) subject data representative of average (panel **A**) and very low (panel **B**) HRV, determined according to the standard deviation of all normal-to-normal intervals (SDNN) of 495 subjects. The ECM is constructed as described by Li et al. [23] and shown in Figure 1. Subjects with diminished HRV exhibit extreme RRI consistency, resulting in the parallel alignment of adjacent R^{n+1}-peaks. Subjects with SDNN values close to the sample mean do not display such striking alignment, due to RRI variation with each heartbeat.

Figure 3. Critically ill patients in the UM-NICU exhibit HRV much lower than that of relatively healthy outpatients from the SHHS. The SDNN was calculated from 5-minute sections of ECG data drawn from 30-minute epochs. ECM was used to facilitate the selection of 5-minute sections of data with minimal artifact contamination within each epoch. Consequently, 5-minute segments were collected in a somewhat irregular fashion within the full recording. SDNN values were computed in this manner for 4 hours of electrophysiological data collected from NICU patients who suffered cardiac arrest less than 24 hours from the time of the recording (n=5). SHHS participants (n=493) were used for comparison; 5-minute SDNN values were imported from SHHS data for analogous 30-minute epochs, with each 4-hour recording beginning at the time of sleep onset. SDNN values for each epoch are reliably diminished in critically ill patients compared to relatively healthy individuals (panel **A**). For a single patient recording of

sufficient duration, 5-minute ECM images were constructed from the twelve hours prior to cardiac arrest. Representative images from Patient D are displayed from various time points during the recording. The patient's time of death was entered at 3:28 PM and loss of signal occurred at 8:42 AM. The time at which each 5-minute segment begins is displayed to the right of each image (panel **B**). **P*<0.05, ***P*<0.01, ****P*<0.001 between groups as determined by two-sample Student's t-test.

Figure 4. ECM-based qualitative HRV evaluation is less sensitive to erroneous algorithmic peak annotation and the presence of arrhythmias. Wrongly detected R peaks are visually apparent and can be corrected before consideration for HRV changes (panel **A**). The positions of the wrongly placed peaks are indicated in the ECG panel (upper) as downward black arrows on three of the heartbeats on the P waves, and in the ECM panel (lower) as the area boxed. The misplaced peaks are visually apparent on ECM display and can be manually corrected if needed. Ectopic contamination with PACs does not significantly disrupt the appearance of diminished HRV (panel **B**). The representative PAC is indicated by a horizontal black bar on the ECG panel (upper) and a black arrow on the ECM panel (lower). There are 6 PACs in this 5-min long ECM epoch, none of which interferes with the HRV inspection on ECM. For this particular segment, the uncorrected SDNN was found to be 35.92 ms. When corrected by simple deletion of the affected RRIs, the true SDNN was found to be 2.31 ms,

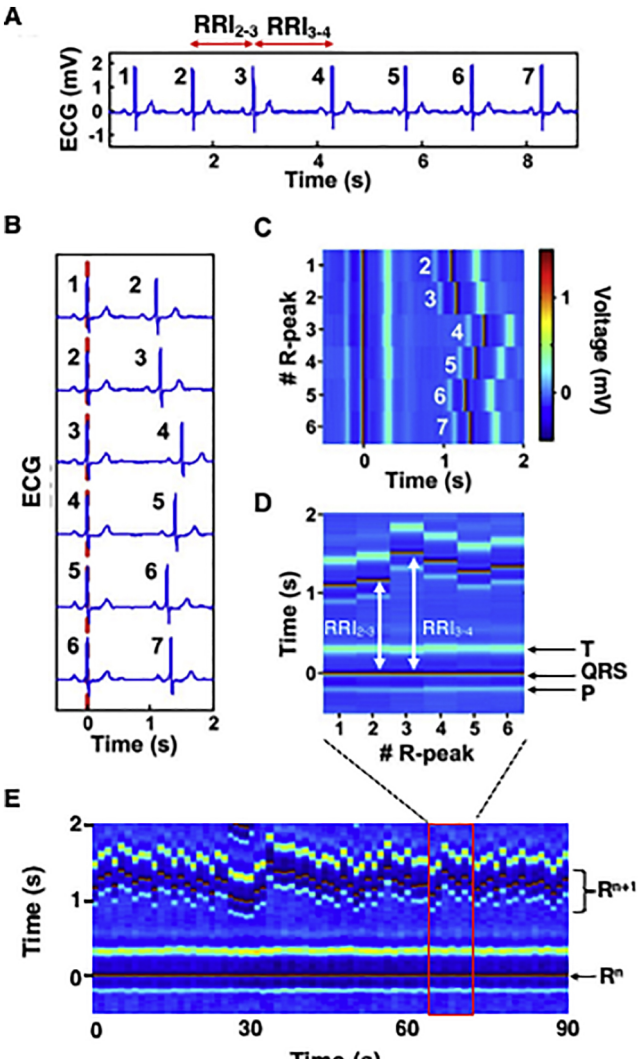
A
RRI2-3 RRI3-4
ECG (mV)
Time (s)
B
ECG
Time (s)
C
R-peak
Time (s)
Voltage (mV)
D
Time (s)
RRI2-3
RRI3-4
T
QRS
P
R-peak
E
Time (s)
Rn+1
Rn

Figure 1

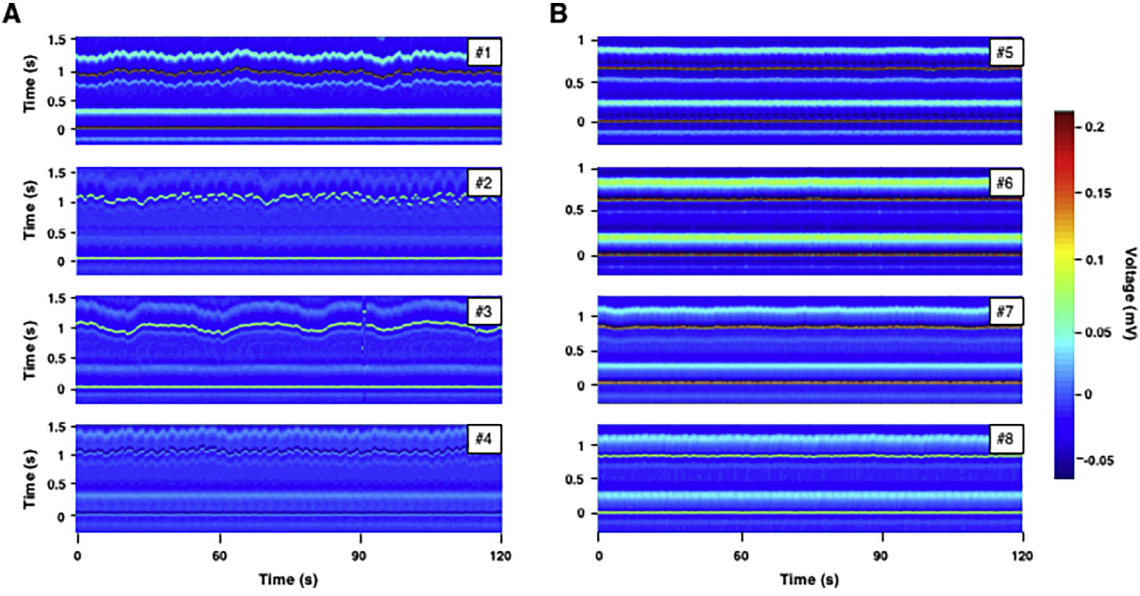
A
B
#1
#2
#3
#4
#5
#6
#7
#8
Time (s)
1.5
1
0.5
0
0
60
90
120
Voltage (mV)
0.2
0.15
0.1
0.05
0
-0.05

Figure 2

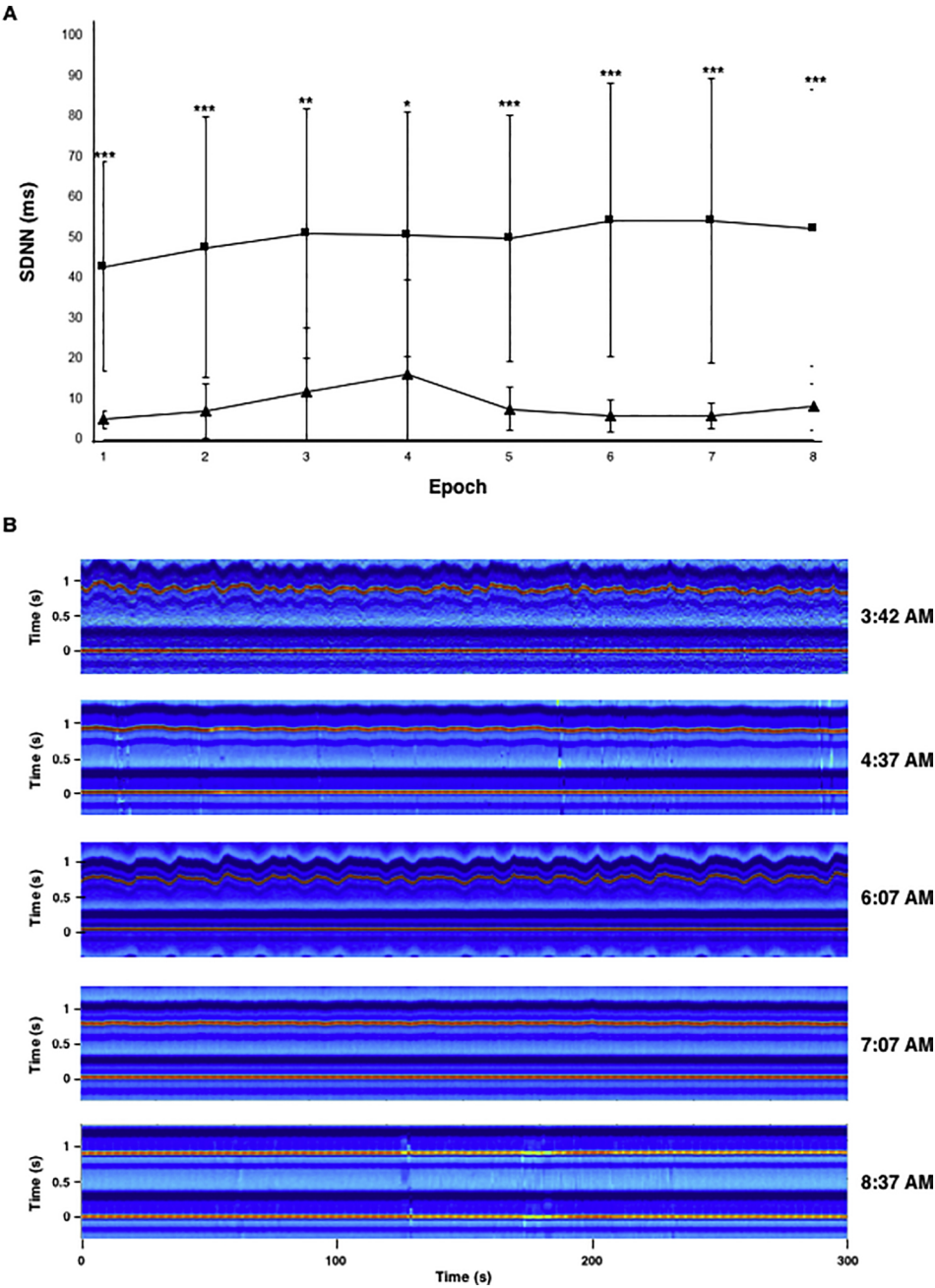

Figure 3

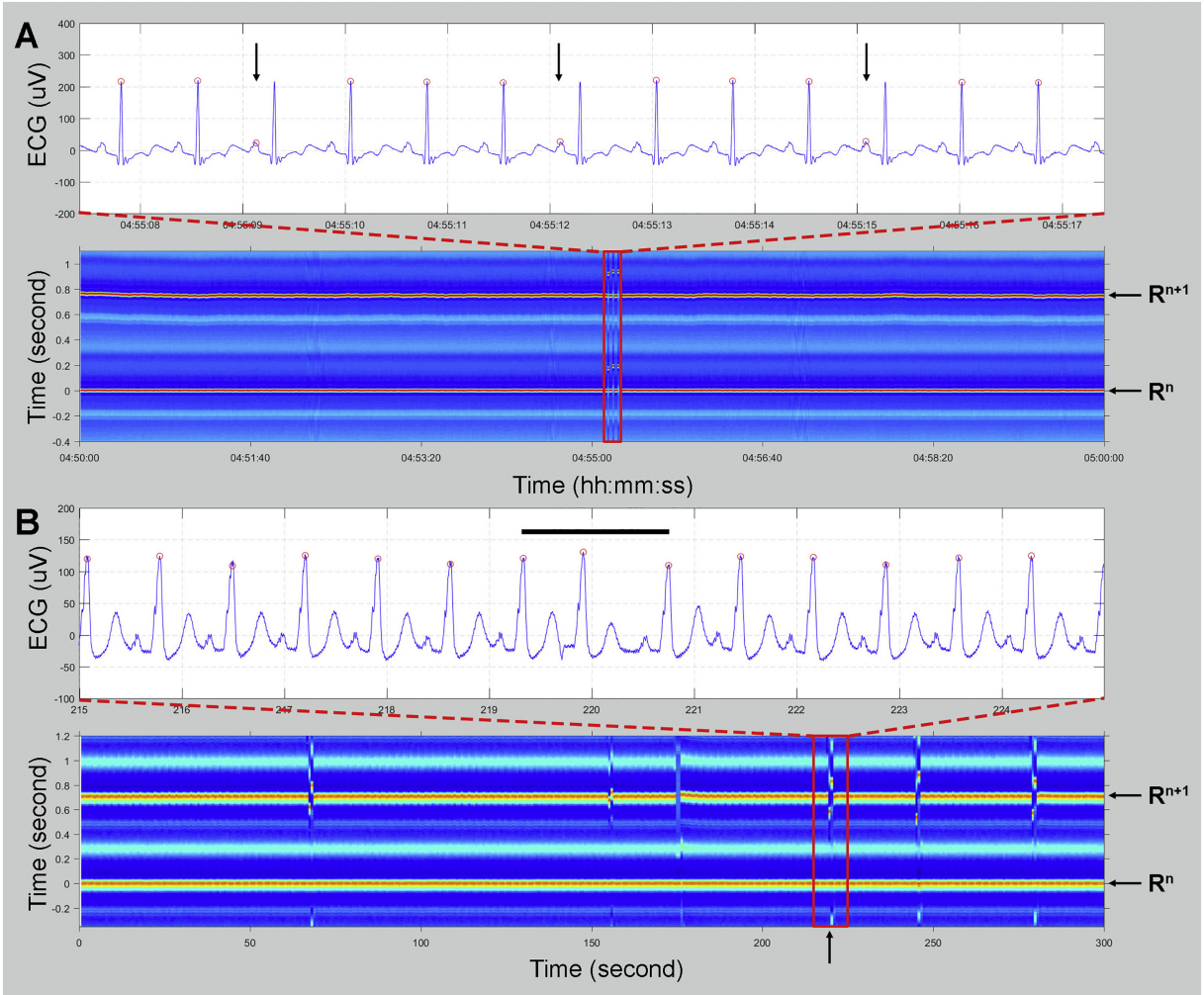
A
ECG (uV)
400
300
200
100
0
-100
-200
04:55:08
04:55:09
04:55:10
04:55:11
04:55:12
04:55:13
04:55:14
04:55:15
04:55:16
04:55:17
Time (second)
1
0.8
0.6
0.4
0.2
0
-0.2
-0.4
R^{n+1}
R^{n}
04:50:00
04:51:40
04:53:20
04:55:00
04:56:40
04:58:20
05:00:00
Time (hh:mm:ss)
B
ECG (uV)
200
150
100
50
0
-50
-100
215
216
217
218
219
220
221
222
223
224
Time (second)
1.2
1
0.8
0.6
0.4
0.2
0
-0.2
R^{n+1}
R^{n}
0
50
100
150
200
250
300
Time (second)

Figure 4